frontiers | Frontiers in Bioengineering and Biotechnology

ORIGINAL RESEARCH
published: 12 April 2022
doi: 10.3389/fbioe.2022.836082

Paper-Based Devices for Capturing Exosomes and Exosomal Nucleic Acids From Biological Samples

Chi-Hung Lai[1], Chih-Ling Lee[1], Cao-An Vu[1], Van-Truc Vu[1], Yao-Hung Tsai[2], Wen-Yih Chen[1] and Chao-Min Cheng[2]**

[1]Department of Chemical and Materials Engineering, National Central University, Taoyuan, Taiwan, [2]Institute of Biomedical Engineering, National Tsing Hua University, Hsinchu, Taiwan

Exosomes, nanovesicles derived from cells, contain a variety of biomolecules that can be considered biomarkers for disease diagnosis, including microRNAs (miRNAs). Given knowledge and demand, inexpensive, robust, and easy-to-use tools that are compatible with downstream nucleic acid detection should be developed to replace traditional methodologies for point-of-care testing (POCT) applications. This study deploys a paper-based extraction kit for exosome and exosomal miRNA analytical system with some quantifying methods to serve as an easy sample preparation for a possible POCT process. Exosomes concentrated from HCT116 cell cultures were arrested on paper-based immunoaffinity devices, which were produced by immobilizing anti-CD63 antibodies on Whatman filter paper, before being subjected to paper-based silica devices for nucleic acids to be trapped by silica nanoparticles adsorbed onto Whatman filter paper. Concentrations of captured exosomes were quantified by enzyme-linked immunosorbent assay (ELISA), demonstrating that paper-based immunoaffinity devices succeeded in capturing and determining exosome levels from cells cultured in both neutral and acidic microenvironments, whereas microRNA 21 (miR-21), a biomarker for various types of cancers and among the nucleic acids absorbed onto the silica devices, was determined by reverse transcription quantitative polymerase chain reaction (RT-qPCR) to prove that paper-based silica devices were capable of trapping exosomal nucleic acids. The developed paper-based kit and the devised procedure was successfully exploited to isolate exosomes and exosomal nucleic acids from different biological samples (platelet-poor plasma and lesion fluid) as clinical applications.

Keywords: paper-based device, exosome, exosomal miRNA, nucleic acid extraction, immunoassay, plasma, wound fluid, colorimetric sensing

OPEN ACCESS

Edited by:
Eden Morales-Narváez, Centro de Investigaciones en Optica, Mexico

Reviewed by:
Kar Wey Yong, University of Alberta, Canada
Tohid Mahmoudi, Tabriz University of Medical Sciences, Iran

****Correspondence:***
Chao-Min Cheng
chaomin@mx.nthu.edu.tw
Wen-Yih Chen
wychen@ncu.edu.tw

Specialty section:
This article was submitted to Nanobiotechnology, a section of the journal Frontiers in Bioengineering and Biotechnology

Received: *15 December 2021*
Accepted: *08 March 2022*
Published: *12 April 2022*

Citation:
Lai C-H, Lee C-L, Vu C-A, Vu V-T, Tsai Y-H, Chen W-Y and Cheng C-M (2022) Paper-Based Devices for Capturing Exosomes and Exosomal Nucleic Acids From Biological Samples. Front. Bioeng. Biotechnol. 10:836082. doi: 10.3389/fbioe.2022.836082

INTRODUCTION

Multivesicular bodies (MVBs), which contain intraluminal vesicles (ILVs) formed by cell membrane invagination, are created intracellularly from the loading of biomolecules into ILVs by the cell of origin. The ILVs are then released from the cells (Akers et al., 2013; Mathieu et al., 2019) and ubiquitously distributed to the bladder, liver, spleen, bone, blood, heart, thyroid, lung, kidney, brain (Betzer et al., 2017; Abello et al., 2019; Faruqu et al., 2019; Rashid et al., 2019; Royo et al., 2019) after integrating with specific sites on the generating cell membrane. In 1889, the British surgeon Paget discovered that tumor cells easily metastasize in multiple -directions to tissues but can only thrive in a favorable microenvironment and

proposed the "seed and soil hypothesis" (Liu et al., 2017). In 2015, Lyden et al. provided more comprehensive data indicating that tumor cells initially release exosomes that are transported to target organs and tissues and taken up by receptors (Hoshino et al., 2015). Exosomes (30–150 nm^{10}), which are nanovesicles surrounded by a lipid bilayer, have recently been discovered to be released by various cells (Qiao et al., 2020; Yan and Jiang, 2020; Kumar et al., 2021; PinkyGupta et al., 2021) and carry an assortment of biological molecules, including proteins, lipids, nucleic acids (miRNA, mRNA, DNA), metabolites, etc. (Qing et al., 2018; Jeppesen et al., 2019; Sharma and Johnson, 2019; Zhang et al., 2019; Kalluri and LeBleu, 2020; Ocansey et al., 2020), which are delivered by cells of origin to specific receptor cells and are essential for the transmission of information between cells. Furthermore, exosomes are capable of influencing tumor growth by regulating immune function, promoting tumor angiogenesis and metastasis, and enhancing drug resistance of cancerous cells (Wan et al., 2018; Mashouri et al., 2019; Sharma and Johnson, 2019; Wortzel et al., 2019). Exosomes have been demonstrated to be highly associated with numerous cancers, including colorectal (Yan et al., 2017), gastric (Huang et al., 2020), liver (Li et al., 2017), lung (Park et al., 2017), pancreatic (Carmicheal et al., 2019), and prostate cancers (Lee et al., 2018). They have the potential for clinical applications and are considered a diagnostic marker to facilitate possible precision treatment.

MicroRNAs (miRNAs), one of the bio-species transported by exosomes, are a group of endogenously small noncoding RNAs that are responsible for posttranslational regulation in cells and play a very profound role in the development of pathology. miRNAs are vital biomarkers for disease diagnosis and prognosis because anomalous expression of miRNAs in cells and exosomes is highly correlated with a variety of human diseases. For example, it has been reported that certain miRNAs can be used as tumor oncogenes and suppressor genes to control cancerous cells and suppress tumor growth, respectively. Although several methodologies have been invented to facilitate precision disease diagnosis point-of-care testing (POCT or bedside testing, a medical analysis performed near the patients (Quesada-González and Merkoçi, 2018)) in developed nations, a number of challenges must be addressed prior to their appropriate application in clinical practice. These obstacles are sample purification difficulties and the need for expensive equipment that restricts rapid and broadly available testing, which is even more difficult to overcome in developing or underdeveloped countries. Therefore, an appropriately simple and robust approach for the rapid extraction of nucleic acids that can be integrated into POCT would significantly impact precision and companion disease diagnosis.

Lab-on-chip (LOC), a description of miniaturized devices at millimeter-to-centimeter scales that integrate single or multiple functions of a laboratory into a chip (Sengupta and Hussain, 2019), is one of two major types of POCT devices (Romao et al., 2017). A category of LOC devices, paper-based analytical devices (PADs), have recently emerged as promising candidates for POCT because of their low cost, simplicity, recyclability, and disposability by incineration (Smith et al., 2018; Hristov et al., 2019). In comparison with conventional instruments, LOC is not only more portable but also can be operated without external power resources (Smith et al., 2018; Hristov et al., 2019). More importantly, it has been demonstrated to potentially fulfill the ASSURED criteria (affordable, sensitive, specific, user-friendly, rapid and robust, equipment-free, and deliverable to end users) proposed by the World Health Organization (WHO) for the development of POCT applications in areas with limited resources (Hu et al., 2014; Smith et al., 2018). Exploiting the rapid growth and recent advances in paper-based technologies for POCT, especially in nucleic acids and immunoassays (Choi et al., 2017; Zhu et al., 2019; Lee et al., 2020; Mahmoudi et al., 2020), this research deployed a novel and easy-to-use technique for sample preparation of exosomal miRNA as biomarker for liquid biopsy by designing a paper-based system, including paper-based immunoaffinity and paper-based silica devices, to capture exosomes derived from HCT116 cells cultured in varied microenvironments and nucleic acids carried by the harvested exosomes. The cells were initially observed by microscopy and the culture media undergoing an ultrafiltration step to concentrate the exosomes and subsequently analyzed by qNano. The paper-based immunoaffinity devices were then employed to capture concentrated exosomes before being undergone lysis buffer and silica-coated papers to trap nucleic acids. The captured exosomes were quantified by enzyme-linked immunosorbent assay (ELISA) and characterized by field-emission scanning electron microscopy (FE-SEM) whereas microRNA 21 (miR-21), a representative target among the exosomal nucleic acids trapped by paper-based silica devices, was determined by quantitative reverse transcription polymerase chain reaction (RT-qPCR) to examine the operability of the developed paper-based system. (**Figure 1**). This system was finally exploited to isolate exosomes and exosomal nucleic acids from various clinical samples (plasma and wound fluid) as a practical application of sample preparation.

MATERIALS AND METHODS

Cell Cultures for Capturing Exosome

HCT116 cancer cells (human colorectal cancer cells) were provided by the Laboratory of Molecular Diagnostics and Therapeutics, Department of Biomedical Sciences and Engineering, National Central University (NCU), Taiwan. The cells were cultured in McCoy's 5A (modified) medium containing 1% penicillin/streptomycin double antibiotic solution and 10% fetal bovine serum (all from Thermo Fisher Scientific, United States) and incubated at 37°C with 5% CO_2 for 3 days. To create different microenvironments, we adjusted the pH value from 7.4 to 6.5 by adding 1 M HCl (ECHO Chemical, Taiwan). The cell morphology was captured at ×100 magnification by a microscopy instrument.

Concentrating HCT116 Cell-Derived Exosomes

Media were collected and centrifuged at 1,200 g for 15 min to remove cells and unwanted contaminants before transferring the supernatant to new containers for centrifugation at 8,000 g in 30 min to remove cell debris. The media were again centrifuged a

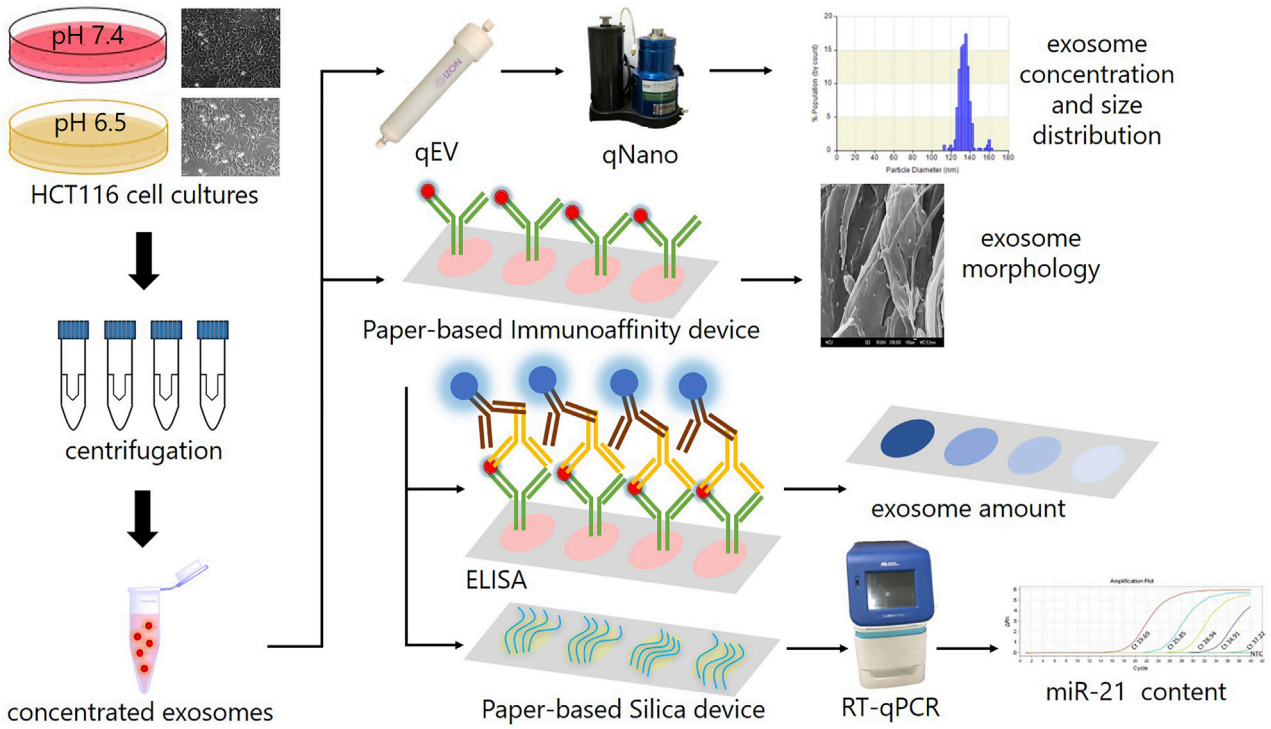

FIGURE 1 | The scheme describes the experimental design in this study. HCT116 cells were cultured in various microenvironments (pH 7.4 and 6.5), characterized by microscope, ultrafiltrated to collect concentrated exosomes, which were then analyzed by a qNano instrument to determine their concentration and size distribution, and subjected to paper-based immunoaffinity devices for exosome capture. The morphology of captured exosomes was subsequently characterized by SEM and their amount was quantified by ELISA. Eventually, exosomal nucleic acids were absorbed by paper-based silica devices for miR-21 quantification by RT-qPCR.

third time at 10,000 g for 30 min in a 10-kDa PES vivaspin concentrate tube (GE Healthcare, UK). The last centrifugation to purify the contents was completed at 10,000 g for 30 min after adding 3 ml PBS. This final suspension was then 1) analyzed by a qNano instrument and 2) used as materials for exosome extraction by paper-based immunoaffinity devices.

Analyzing the Size Distribution of Concentrated Exosomes by qNano

The size distribution of the exosomes captured from cell cultures was analyzed by a qNano Particle Analyzer (IZON, Science New Zealand) after pretreatment with a qEV size exclusion chromatography (SEC) column (IZON, Science New Zealand). The nanopore setting was employed on the qNano, and 75 µL PBS was added. The stretch was set to 47 mm, the operating voltage was set to 0.74 V, and the pressure was set to 12 cm H_2O. Sample size was determined via calibration with standard beads of known size.

Fabrication of Paper-Based Immunoaffinity Devices to Capture Exosomes

The paper-based immunoaffinity devices were produced by immobilizing anti-CD63 antibodies on grade 1 Whatman filter papers (**Supplementary Figure S2**). Initially, the targeted reaction zone of this substrate was treated with 50 µL of 4% (v/v) 3-mercaptopropyl tri-methoxysilane (Sigma-Aldrich, United States) in 99% ethanol (ECHO chemical, Taiwan) and incubated for 30 min. Subsequently, the reaction zone was treated with 50 µL of N-γ-maleimidobutyryloxy succin-imide ester (GMBS) (Thermo Scientific, United States) (0.01 µmol in 99% ethanol) and incubated for 15 min. The device was then incubated in 10 µg/ml Neu-trAvidin (Thermo Scientific, United States) solution in PBS (Thermo Scientific, United States) at 4°C for 1 h. Blocking was conducted with 1% (w/v) bovine serum albumin (BSA) (Sigma-Aldrich, United States) in phosphate-buffered saline (PBS) for 10 min and repeated 3 times. Finally, the reaction zone was introduced with 20 µL of biotinylated mouse anti-human anti-CD63 antibody (BioLegend, United States) and incubated for 10 min 3 times.

Characterization of Captured Exosomes by Field-Emission Scanning Electron Microscopy (FE-SEM)

The exosomes captured by the paper-based immunoaffinity device were treated with 20 µL of mixed paraformaldehyde (PFA) (Sigma-Aldrich, United States) and incubated with glutaraldehyde (GA) (Sigma-Aldrich, United States) in PBS buffer for 30 min at room temperature before being washed

3 times with PBS. In the next steps, the sampled zone was dehydrated by 20 μL of 50% ethanol in 15 min, followed by 75, 87.5, 93.75, and 99% ethanol for 10 min each. Eventually, 20 μL of 99% ethanol was applied and allowed to dry at room temperature for 30 min. The resulting samples were examined by a JSM-7500F FE-SEM (JEOL Japan).

Quantification of Captured Exosomes by ELISA on Paper-Based Immunoaffinity Devices (P-ELISA)

Determining the exosome content by P-ELISA was accomplished by initially adding 20 μL analyte to the paper-based immunoaffinity devices and incubating for 1 h. Subsequently, the devices were treated with 5 μL of rabbit anti-human anti-CD9 antibody (1 μg/ml in PBS from Sigma-Aldrich, United States) and incubated for 1 min before being washed 3 times with 20 μL PBS. A similar procedure of adding-incubating-washing was duplicated on the device with 5 μL of HRP-conjugated goat anti-rabbit antibody (Sigma-Aldrich, United States). Finally, 5 μL of mixed 3,3′,5,5′-tetramethylbenzidine (TMB) (Sigma-Aldrich, United States) and hydrogen peroxide (Sigma-Aldrich, United States) (1:1 mix per volume) was added, and the device was incubated for color development (**Supplementary Figure S3**). The P-ELISA results were photographed with a cell phone camera (iPhone XR) in 8-bit format, and the color intensity from the last reaction step was quantified by ImageJ software.

Adsorption of Exosomal Nucleic Acids by Paper-Based Silica Devices

Paper-based silica devices were prepared by adding 20 μL silica nanoparticle solution (Sigma-Aldrich, United States) (3 mg/ml) to both sides of grade 1 Whatman filter papers before drying at room temperature for 20 min. The exosome lysate, obtained by incubating paper-based immunoaffinity devices after capturing exosomes with RNase-free water as lysis buffer at 95°C for 30 min, was then placed on paper-based silica devices at room temperature for 3 min for nucleic acid absorption (**Supplementary Figure S4**). Eventually, the paper-based silica devices containing attached nucleic acids were treated with RNase-free water as an elution buffer at 55°C for 45 min to collect exosomal nucleic acid solutions.

Quantifying Exosomal miR-21 by RT-qPCR

Reverse transcription of miR-21 complementary DNA (cDNA) (by TaqMan™ MicroRNA Reverse Transcription kit from Thermo Scientific - United States) and qPCR (by QuantiFast SYBR® green PCR kit from Qiagen—Germany; with the probes and primers shown in (**Supplementary Table S1**) were conducted to quantify the content of this RNA in exosomal nucleic acid solution. In detail, 10.2 μL of a solution composed of 1 μL of exosomal nucleic acid, 1 μL of 10x Poly(A)pol reaction buffer, 1 μL of 1 mM Adenosine 5′ Triphosphate, 1 μL of 1 mM deoxynucletide (dNTP) Solution Mix, 1 μL of 10 μM RT primer, 0.5 μL of SuperScript® III reverse transcriptase, 0.2 μL of *E. coli* Poly(A) polymerase, 0.2 μL of rnase inhibitor (20 U/μL), and 4.3 μL of nuclease-free water was incubated at 42°C for 1 h before increasing the temperature to 95 °C for 5 min to inactivate the enzyme and facilitate the collection of exosomal RT cDNA. One microliter of the resulting RT cDNA, 1 μL of each primer (1.5 μM), and 5 μL of 2× QuantiFast SYBR Green PCR Master Mix (Qiagen) were dissolved in 2 μL of deionized water for qPCR, which was performed by a StepOnePlus real-time PCR system (Applied Biosystem, United States). This process was initiated at 95 °C for 5 min, followed by 40 cycles at 95°C for 10 s and finished at 60°C for 30 s. The amplification plots and melting curves were generated using StepOne software v2.3.

Applying the Paper-Based Kit to Capture Exosomes and Exosomal Nucleic Acids From Clinical Samples

Platelet-poor plasma (PPP) and fluidic samples of chronic lesion tissues, obtained from various patients at different times of curing progress and provided by Dr. Shin-Chen Pan—Department of Plastic Surgery, affiliated hospital of National Cheng Kung University (IRB No. B-ER-109-238), were used as clinical samples to validate the applicability of the fabricated devices. The wound fluid was directly undergone the paper-based kit without pretreatment whereas the PPP samples were separated by a sequential membrane system with pore sizes of 200 and 30 nm (**Supplementary Figure S5**). Theoretically, the vast majority of exosomes with a reported diameter within 30–200 nm are retained in the space between two membrane layers (Retention sample) while a minority of them can penetrate the 200-nm filtration (Filtrate sample). Exosomal miR-21 harvested from all of these clinical samples by the paper-based kit was eventually determined and evaluated via Ct values comparison. Three plasma-derived samples (PPP, Retention, and Filtrate) were also examined by Nanoparticle Tracking Analysis (NTA) as an assistance for assessing the RT-qPCR data (**Supplementary Table S2**).

RESULTS AND DISCUSSIONS

Characterizing Cells Cultured in Various Microenvironments

The capability of paper-based devices developed in this study were examined by employing them for capturing and quantifying exosomes and exosome-derived nucleic acids from cells cultured in different microenvironments. To do this, HCT116 - a human colorectal cancer cell line - was initially cultured in pH 7.4 medium before gradually altering this parameter to 7.2, 6.9, 6.7, and 6.5. The final products from the media at pH 7.4 and 6.5 were observed by microscopy (**Figure 2**), which showed that there were few differences in morphology between cells cultured in microenvironments with pH 7.4 (**Figures 2A–D**) and 6.5 (**Figures 2E–H**), suggesting that it is feasible to harvest exosomes from cells cultured in various microenvironments.

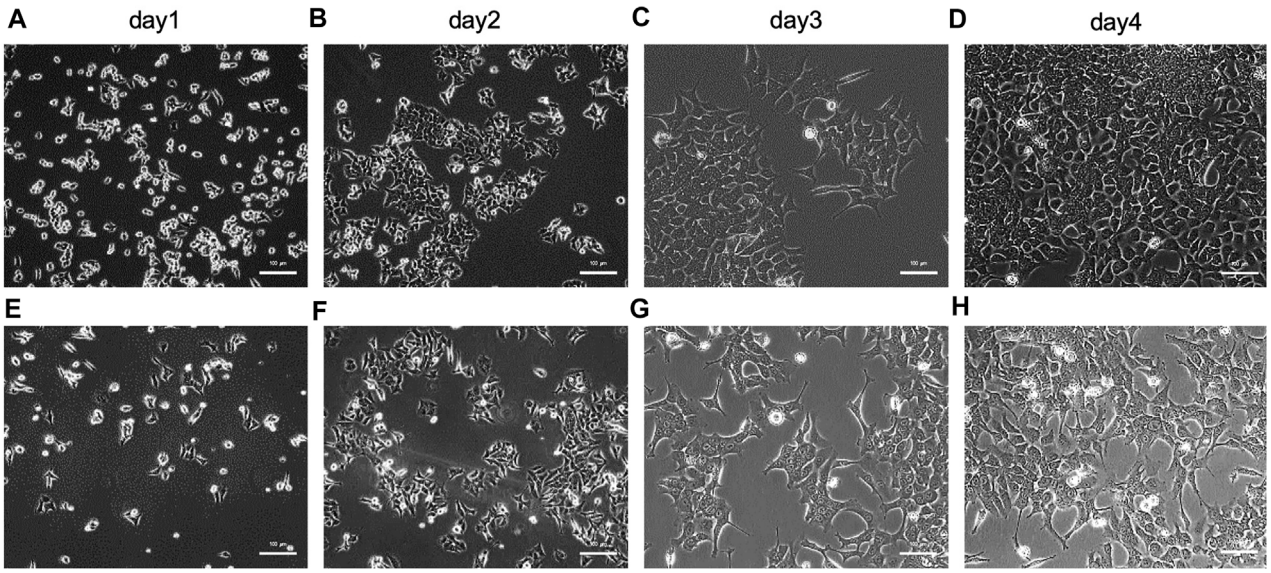

FIGURE 2 | Characterization of HCT116 cells cultured in various microenvironments of **(A)**~**(D)** pH 7.4 after **(A)** 1, **(B)** 2, **(C)** 3, and **(D)** 4 days, and **(E)**~**(H)** pH 6.5 after **(E)** 1, **(F)** 2, **(G)** 3, and **(H)** 4 days by microscope. The scale bar is 100 μm.

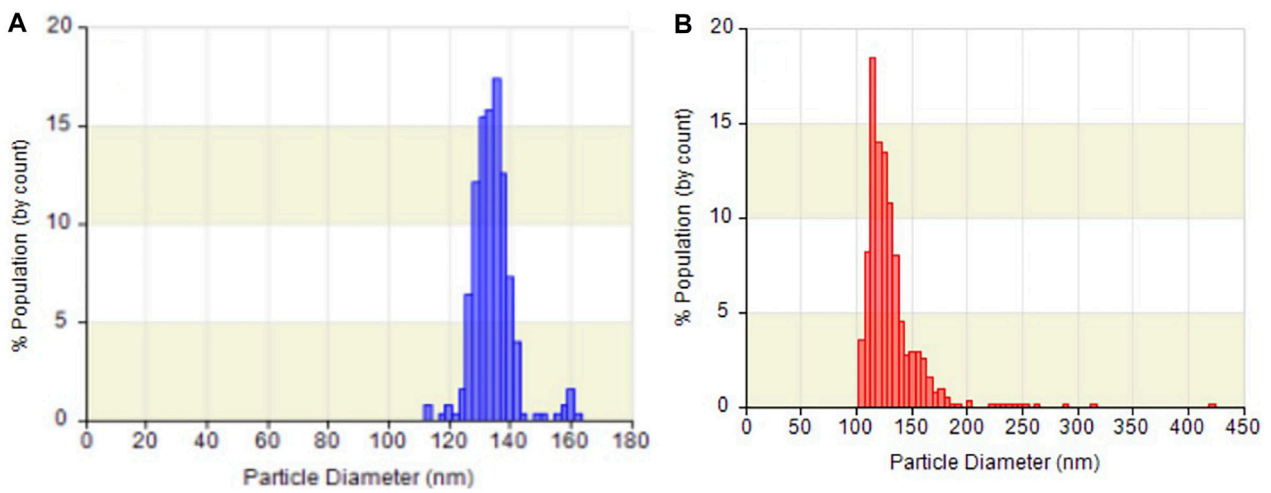

FIGURE 3 | Particle size distribution and concentration of **(A)** exosomes from HCT116 cell culture medium and **(B)** commercial lyophilized exosomes analyzed by qNano.

Size Distribution, Concentration, and Characteristics of HCT116 Cell-Derived Exosomes

Exosomes, with a particle size of 30–150 nm encapsuled by a lipid bilayer and a concentration of approximately 10^8 particles/mL in cell culture media (He et al., 2018; Heinemann et al., 2014), are essentially guaranteed not to be damaged during centrifugation prior to quantification by ELISA, and these exosomes were used as materials for nucleic acid extraction. Hence, the size distribution and concentration of HCT116 cell-derived exosomes in the pretreated media were statistically characterized by the qNano instrument after being ultra-filtrated, and their particle morphology was examined by FE-SEM after being captured by paper-based immunoaffinity devices. On the one hand, concentrations of 3.6×10^8 exosomes/mL and size distributions of approximately 110–160 nm (mean diameter of 133.1 nm, **Figure 3A**) were observed, which was equivalent in amount and identical in size to those of the standard sample (3.4×10^9 exosomes/mL and 100–200 nm (mean diameter of 129 nm, **Figure 3B**) identified from a 1.9×10^9 exosome/mL solution of commercially

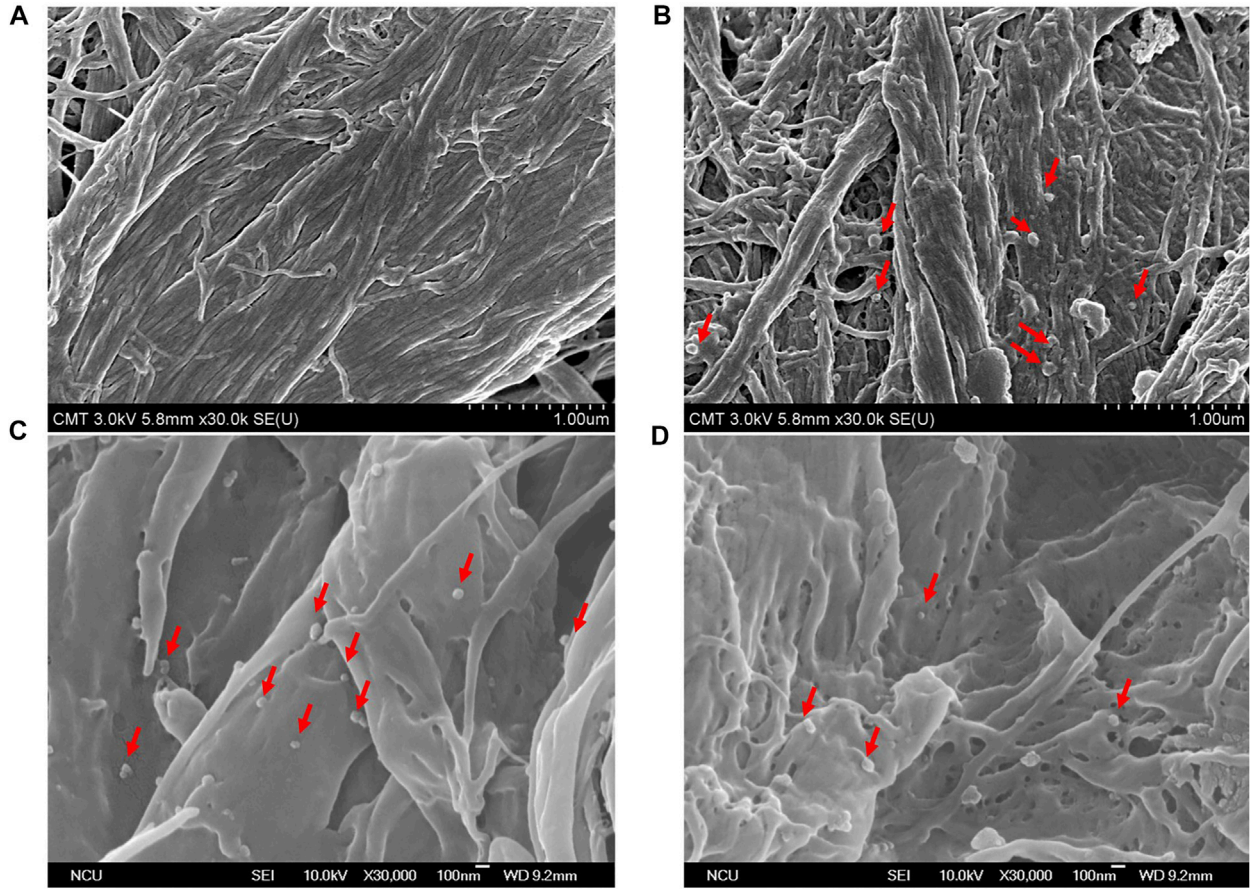

FIGURE 4 | SEM pictures characterize surface morphology of **(A)** untreated sample, **(B)** commercial lyophilized exosomes, and **(C,D)** HCT116-derived exosomes captured by paper-based immunoaffinity devices. Red arrows indicate captured exosomes.

available lyophilized exosomes from the HCT116 cell line (human colon carcinoma) obtained from Hansa BioMed Life Science, Estonia), indicating that HCT116 cell-derived exosomes pretreated by our proposed method met the commercial requirements. On the other hand, exosome-like particles (Enderle et al., 2015; Wu et al., 2015) appeared in the SEM images of the media isolated by the designed system (**Figures 4C, D**) in comparison with the SEM images of the blank sample (**Figure 4A**); these particles had round and cup shapes and dimensions equivalent to those of the commercial products (**Figure 4B**), confirming that the immunoaffinity devices fabricated in this study succeeded in capturing exosomes and therefore is applicable for further purposes.

Quantifying Exosomes Captured on Paper-Based Immunoaffinity Devices by ELISA (P-ELISA)

In the next step, P-ELISA (described in experimental section) was used for the quantification of exosomes captured from cells cultured in the aforementioned microenvironments. The data presented in **Figure 5** demonstrated that the paper-based immunoaffinity devices were capable of seizing exosomes at different contents, in which the color intensified with increasing concentrations of exosomes (**Figure 5**). A calibration line (y = 25.4x - 191) was therefore constructed to formulate the relationship between the exosome levels ($\log_{10}$ values, x) and the color intensity (y) (inset of **Figure 5**). Since the color intensities observed in the samples from the pH 7.4- and 6.5-pretreated media were statistically distinguishable (p value <0.05) and within the linear region of the calibration line, the exosome concentrations of these two varied microenvironments were estimated to be 1.53×10^8 and 2.05×10^8 exosomes/mL, respectively. These empirical figures not only indicated that cancerous cells released more exosomes in acidic microenvironments than in neutral microenvironments, which is identical to a discovery reported by several groups (Parolini et al., 2009; Logozzi et al., 2017; Boussadia et al., 2018; Logozzi et al., 2018; Tian et al., 2019), but also was an evidence proving that the designed paper-based immunoaffinity devices could effectively determine exosome amounts released in different microenvironments.

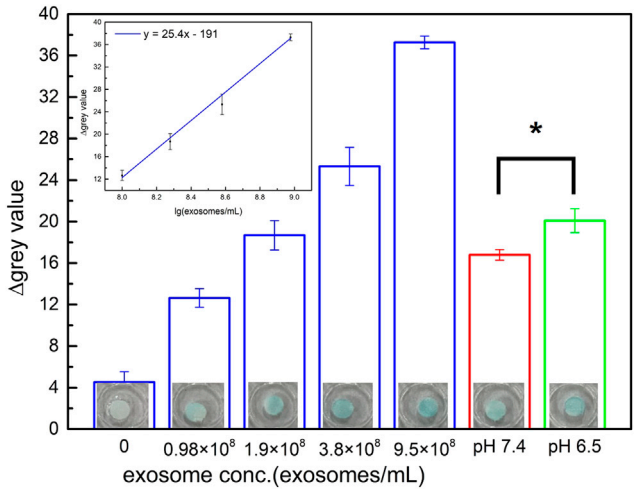

FIGURE 5 | Quantification of exosomes performed by color intensity assessment including commercial lyophilized samples (blue columns) and exosomes captured from the medium of HCT116 cells cultured in various microenvironments of pH 7.4 (red column) and 6.5 (green column). Inset is the calibration curve of exosomes from commercial samples (blue columns). An asterisk (*) denotes a p value <0.05 (obtained from t-test). All of the results were obtained by P-ELISA.

Extracting Exosomal Nucleic Acids From HCT116 Cells Cultured in Various Microenvironments and Determining miR-21 Content by RT-qPCR

Exosomes contain a variety of molecular contents, including proteins and nucleic acids, that can be used to provide cellular information (Qing et al., 2018; Jeppesen et al., 2019; Zhang et al., 2019; Kalluri and LeBleu, 2020; Ocansey et al., 2020; Qiao et al., 2020). Paper-based silica devices can be combined with paper-based immunoaffinity devices to capture exosomal nucleic acids and have extensive applications of POCT. Herein, miR-21, a noncoding RNA of 20–24 nucleotides and among exosomal nucleic acids trapped by paper-based silica devices, was chosen as the representative target because it plays important roles in cell growth, metastasis, and chemoresistance in breast, colorectal, lung, liver, pancreatic, and prostate cancer (Bautista-Sánchez et al., 2020), such that miR-21 can be classified as a cancer "oncomiR" (He et al., 2017; Moscetti et al., 2019).

Numerous patients have been diagnosed with advanced stages of colorectal cancer, which is highly prevalent and has a high mortality rate (Tsukamoto et al., 2017). In recent years, miRNAs have been discovered to be enriched in exosomes prior to being released to body fluids (Li et al., 2015; Zhao et al., 2015). miRNAs encapsulated in exosomes are more stable in body fluids because the exosomal lipid bilayer membrane protects miRNAs from degradation by rnase (Ge et al., 2014; Bhome et al., 2017). There is evidence of significantly higher exosomal miR-21 contents in the serum of colorectal cancer patients than in that of healthy individuals, and some evidence suggests the relation of miR-21 levels to various stages of this cancer (Jin et al., 2019). Activity and concentration of miR-21, which are strongly related to tumor size, stage, and lymph node metastasis, are higher in colorectal cancerous tissues than in normal tissues and decrease in patients after completion of cancer treatment (Tsukamoto et al., 2017; Moridikia et al., 2018). These results indicate that exosomal miR-21 could be used as a biomarker for cancer diagnosis as well as extracting and detecting miR-21 may facilitate effective treatment to reduce mortality.

In this experiment, RT-qPCR was utilized to determine miR-21 and examine the ability of paper-based silica devices in trapping exosomal nucleic acids. After being treated with RNase-free lysis buffer at 95°C for 30 min, the samples were incubated with paper-based silica devices for nucleic acid adsorption before the silica-coated areas were treated with RNase-free elution buffer at 55°C water for 45 min to extract trapped nucleic acids and quantify miR-21 content by RT-qPCR. An investigation of the incubation step was implemented to identify the optimal operating time for nucleic acid adsorption. Empirical results reveal that despite equivalent Ct values (threshold cycle) obtained after the periods of 1, 3, 5, and 10 min, incubating the silica devices with the pretreated samples for 3 min provides the maximal efficiency in terms of time **Supplementary Figure S4**). The subsequent samples were therefore incubated with paper-based silica devices for 3 min to trap synthetic miR-21 at various concentrations to conduct a standard calibration line (**Figure 6A**) which was then used to calculate the miR-21 content in the exosomes from two microenvironments (**Figures 6B, C**). The high Ct values of 10 ml samples in the aforementioned microenvironments not only were not significantly different to each other ($p > 0.05$) (**Figure 6B**) but also revealed low miR-21 levels (**Figure 6C**), which would reduce RT-qPCR fidelity. The initial medium volumes were hence doubled to 20 ml to guarantee the analysis by RT-qPCR. As a result, the theoretical value of ΔCt (the change in Ct values between the initial volume of 10 ml and the final volume of 20 ml) should be 1. On the one hand, the estimated ΔCt of HCT116 in the pH 6.5 microenvironment was 1.56, which is similar to the 9.5 × 10 (Liu et al., 2017) exosomes/mL standard exosomes, demonstrating a significant difference compared to the 10-ml volume sample (p value <0.001). On the other hand, the low ΔCt (approximately 0.21) in the pH 7.4 microenvironment suggested a low RT-qPCR detection fidelity due to the small content of exosomal miR-21. The ΔCt of different initial sample volumes matches the theoretical value of miR-21 quantification by RT-qPCR, indicating that the adsorption process could sufficiently capture exosomal nucleic acids from samples of cells cultured in different media for quantification. U6 siRNA, a small RNA commonly used as a cell content control because of its intracellular origin, was used to guarantee that both exosomes and exosomal nucleic acids were secreted from equal amounts of HCT116 cells cultured in each microenvironment. U6 siRNA was amplified via RT-qPCR and TaqMan® MicroRNA assay after this nucleic acid had been extracted from the products harvested after culturing cells for 3 days in various pH conditions (following identical procedure of culturing HCT116 cells). The Ct values obtained for U6 siRNA derived from U6 cells grown in pH 6.5 and 7.4 media for 3 days were 19.80 and 19.25, respectively (**Figure 6D**), demonstrating that the cell contents in the two examined microenvironments

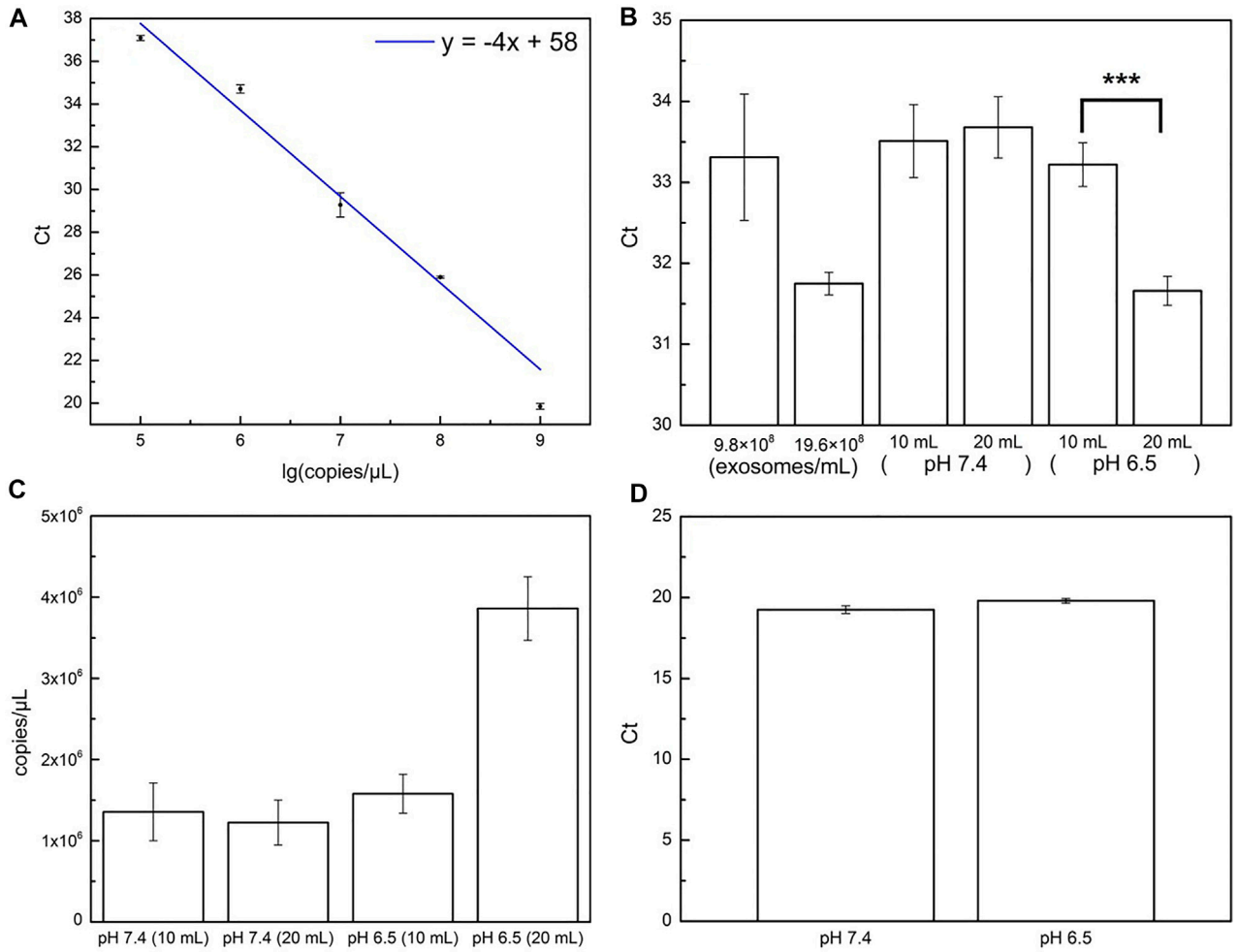

FIGURE 6 | Quantification of miR-21. **(A)** Calibration curve for standard miR-21 samples by paper-based silica devices and quantified by RT-qPCR. **(B)** miR-21 contents (estimated by Ct values) in exosomes from standard samples and from 10 to 20 ml pH HCT116 samples cultured in pH 7.4 and pH 6.5 microenvironments. Three asterisks (***) denote a *p* value <0.001 (obtained from *t*-test). **(C)** miR-21 concentrations (copies/μL) of 10 and 20 ml HCT116 samples cultured in pH 7.4 and pH 6.5 microenvironments, calculated from calibration line in **(A)** and corresponding Ct values in **(B)**. **(D)** U6 SiRNA contents (estimated by Ct values) derived from HCT116 cells cultured in pH 7.4 (red column) and pH 6.5 (green column) conditions.

were equivalent, although the amount in the pH 6.5 medium was slightly lower than that in the pH 7.4 medium because of the slightly higher Ct value in sample of pH 6.5 medium compared to that in the sample of pH 7.4 medium. A comparison between **Figure 5** and **Figure 6** (B and C) not only confirms that HCT116 cells cultured in an acidic environment secreted more exosomes and corresponding miR-21 but also proves that paper-based immunoaffinity and paper-based silica devices were applicable for successful and sensitive extraction.

Extracting Exosomal miR-21 From Biological Samples by Paper-Based Devices

In this section, plasma and wound fluid were used as biological samples to evaluate the clinical applicability of the deployed system. Three plasma-derived samples (PPP, Retention, and Filtrate), formed after filtering PPP with two membranes, were applied on paper-based immunoaffinity and paper-based silica devices for nucleic acid capture (**Supplementary Figure S5**). Their exosomal miR-21 contents were then analyzed by qRT-qPCR and compared with no template control (NTC) sample (**Figure 7A**). Evidently, Ct value achieved from Filtrate was remarkably higher than others and close to that value of NTC, indicating that exosomes are scarcely present in Filtrate. On the other hand, there was only a slight difference between the Ct values of Retention and PPP, suggesting an approximately equal amount of exosomal miR-21 extracted, which is also consistent with the output by NTA in terms of exosome concentrations (**Supplementary Table S2**). These results are, on one hand, reasonable in the context of the possible presence of undesirable molecules of the same sizes as well as exosome loss during filtration that cause NTA measurement error. On the other hand, low exosomal miR-21 counts (high Ct values) in spite of abundant exosomes are congruent with the samples from healthy

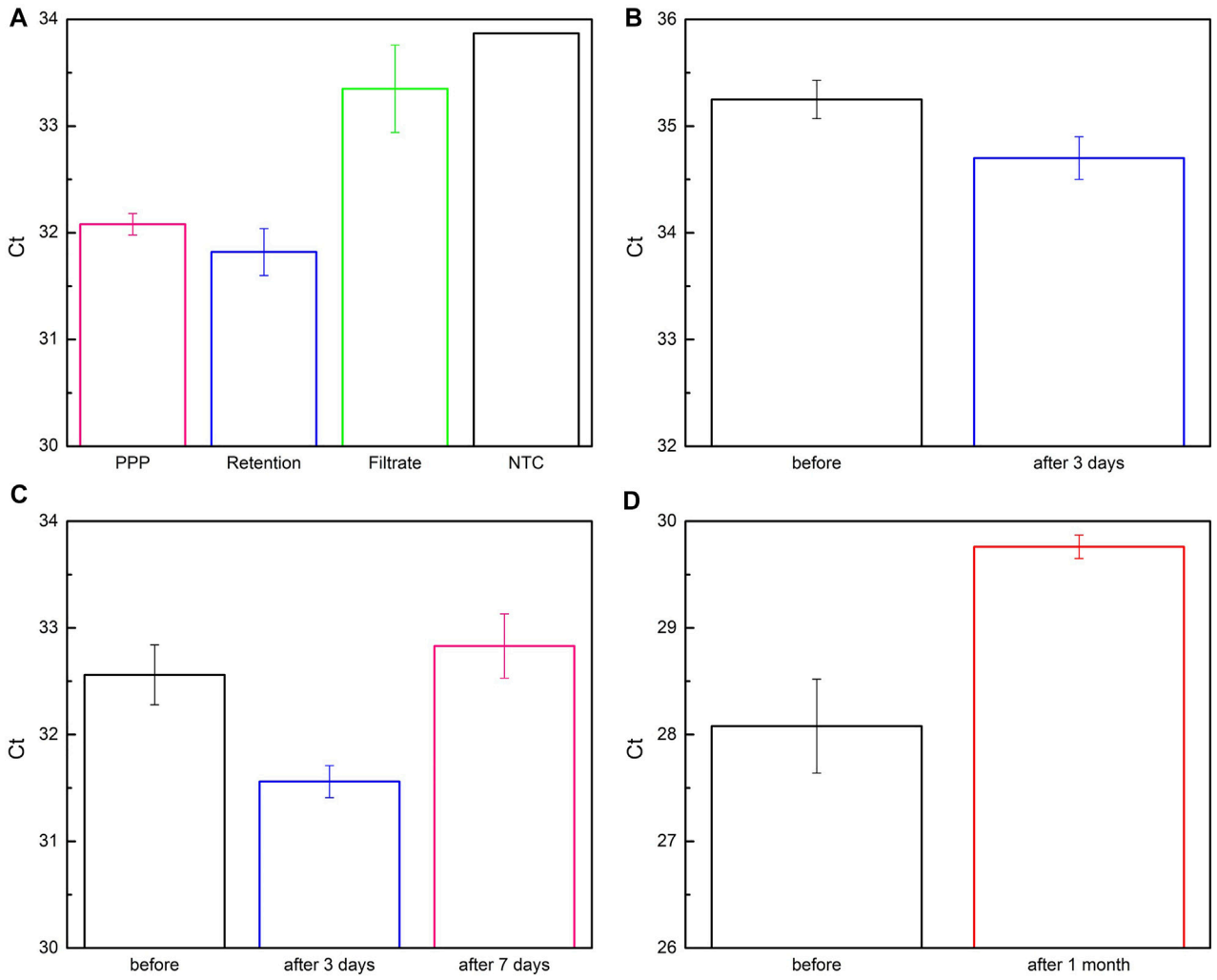

FIGURE 7 | Quantification of exosomal miR-21 from bio-samples captured by paper-based system. **(A)** Plasma-derived samples were obtained by flowing platelet-poor plasma (PPP, pink column) through 200 nm- and 30 nm-membrane to collect Retention (blue column) and Filtrate (green column) samples, respectively. No template control (NTC) was for comparison and analysis. **(B–D)** Fluidic samples were obtained from lesions of patients before and after being monitored for **(B)** 3 days, **(C)**, 7 days, and **(D)** 1 month.

plasma. It is also important to note that the working yield of the paper-based kit in the PPP sample was comparable with the Retention sample (inferred from their equivalent Ct values), even though the PPP was not pre-filtered by two layers of the membrane system to eliminate the interferences from the particles with dimensions outside the range of exosomes. These results indicate that the developed paper-based kit is feasibly combined with sequential membranes for capturing exosomes and exosomal nucleic acids from complex clinical bio-samples.

Encouraged by successful trials with PPP under the facilitation of a sequential membrane system, we furtherly assessed the aptitude of two paper-based devices without assistance by applying them for wound fluid, a more complicated sample than PPP with cells, red blood cells, bacteria, etc. Fluidic samples secreted from chronic lesions before and after 3-day, 7-day, and 1-month surveillance were collected and investigated by comparing the Ct values of miR-21 after RT-qPCR (**Figures 7B–D**), since miR-21 has been reported to be greatly involved in wound healing process (Herter and Xu Landén, 2017). It is noteworthy that exosomal miR-21 expression is distinctly elevated in preliminary phase of the wounds (3 days in **Figures 7B, C**) compared to the longer periods (7 days in **Figures 7C**, 1 month in **Figure 7D**). Its content started reducing after 7 days (**Figure 7C**) and considerably declined after 1 month (**Figure 7D**) when the lesions had been widely swollen and ulcerated. This tendency implied a relationship between exosomal miR-21 and the severity of the lesions as well as raised a hypothesis that exosomal miR-21 not only promotes wound healing but also serves as a biomarker for monitoring and predicting treatment efficacy. These observations were in good agreement with previous investigations, indicating that miR-21 plays a role in healing wound as documented in

the literature (Herter and Xu Landén, 2017). In short, these results demonstrated that the paper-based kit was competent for capturing exosomes and exosomal miR-21 in various types of biological samples.

CONCLUSION

In this study, the designed paper-based system, comprising of paper-based immunoaffinity devices and paper-based silica devices, has successfully captured exosomes and exosomal nucleic acids from a variety of biological samples with easy operation and high efficiency. The paper-based immunoaffinity devices proved that there were more exosomes released by HCT116 cells cultured under acidic conditions than by HCT116 cells cultured under neutral conditions, which is correspondent with higher levels of miR-21 trapped by the paper-based silica devices. The developed kit also succeeded in isolating exosomes and exosomal nucleic acids from PPP and lesion fluids as clinical applications. They can be used alone or in association with another filtration technique. This approach with thin papers therefore not only provides a novel method for capturing exosomes and nucleic acids without requiring expensive equipment, chemicals, extensive training or professional support but also holds great potential to integrate into POCT applications, especially in areas or countries with low resources.

DATA AVAILABILITY STATEMENT

The raw data supporting the conclusion of this article will be made available by the authors, without undue reservation.

AUTHOR CONTRIBUTIONS

C-HL, W-YC and C-MC contributed to conception and design of the work. C-HL, C-LL, C-AV and V-TV acquired and interpreted the data. All the authors analyzed the data. C-HL, C-LL, C-AV, W-YC and C-MC drafted the work and substantively revised it.

ACKNOWLEDGMENTS

The authors acknowledge the financial support from the Ministry of Science and Technology, Taiwan (Grant No. 109-2811-E-008-518) for this research.

SUPPLEMENTARY MATERIAL

The Supplementary Material for this article can be found online at: https://www.frontiersin.org/articles/10.3389/fbioe.2022.836082/full#supplementary-material

REFERENCES

Abello, J., Nguyen, T. D. T., Marasini, R., Aryal, S., and Weiss, M. L. (2019). Biodistribution of Gadolinium- and Near Infrared-Labeled Human Umbilical Cord Mesenchymal Stromal Cell-Derived Exosomes in Tumor Bearing Mice. *Theranostics* 9, 2325–2345. doi:10.7150/thno.30030

Akers, J. C., Gonda, D., Kim, R., Carter, B. S., and Chen, C. C. (2013). Biogenesis of Extracellular Vesicles (EV): Exosomes, Microvesicles, Retrovirus-like Vesicles, and Apoptotic Bodies. *J. Neurooncol.* 113, 1–11. doi:10.1007/s11060-013-1084-8

Bautista-Sánchez, D., Arriaga-Canon, C., Pedroza-Torres, A., De La Rosa-Velázquez, I. A., González-Barrios, R., Contreras-Espinosa, L., et al. (2020). The Promising Role of miR-21 as a Cancer Biomarker and its Importance in RNA-Based Therapeutics. *Mol. Ther. - Nucleic Acids* 20, 409–420. doi:10.1016/j.omtn.2020.03.003

Betzer, O., Perets, N., Angel, A., Motiei, M., Sadan, T., Yadid, G., et al. (2017). *In Vivo* Neuroimaging of Exosomes Using Gold Nanoparticles. *ACS Nano* 11, 10883–10893. doi:10.1021/acsnano.7b04495

Bhome, R., Goh, R. W., Bullock, M. D., Pillar, N., Thirdborough, S. M., Mellone, M., et al. (2017). Exosomal microRNAs Derived from Colorectal Cancer-Associated Fibroblasts: Role in Driving Cancer Progression. *Aging* 9, 2666–2694. doi:10.18632/aging.101355

Boussadia, Z., Lamberti, J., Mattei, F., Pizzi, E., Puglisi, R., Zanetti, C., et al. (2018). Acidic Microenvironment Plays a Key Role in Human Melanoma Progression through a Sustained Exosome Mediated Transfer of Clinically Relevant Metastatic Molecules. *J. Exp. Clin. Cancer Res.* 37, 245. doi:10.1186/s13046-018-0915-z

Carmicheal, J., Hayashi, C., Huang, X., Liu, L., Lu, Y., Krasnoslobodtsev, A., et al. (2019). Label-free Characterization of Exosome via Surface Enhanced Raman Spectroscopy for the Early Detection of Pancreatic Cancer. *Nanomedicine: Nanotechnology, Biol. Med.* 16, 88–96. doi:10.1016/j.nano.2018.11.008

Choi, J. R., Yong, K. W., Tang, R., Gong, Y., Wen, T., Li, F., et al. (2017). Advances and Challenges of Fully Integrated Paper-Based Point-of-care Nucleic Acid Testing. *Trac Trends Anal. Chem.* 93, 37–50. doi:10.1016/j.trac.2017.05.007

Enderle, D., Spiel, A., Coticchia, C. M., Berghoff, E., Mueller, R., Schlumpberger, M., et al. (2015). Characterization of RNA from Exosomes and Other Extracellular Vesicles Isolated by a Novel Spin Column-Based Method. *Plos One* 10, e0136133. doi:10.1371/journal.pone.0136133

Faruqu, F. N., Wang, J. T.-W., Xu, L., McNickle, L., Chong, E. M.-Y., Walters, A., et al. (2019). Membrane Radiolabelling of Exosomes for Comparative Biodistribution Analysis in Immunocompetent and Immunodeficient Mice - a Novel and Universal Approach. *Theranostics* 9, 1666–1682. doi:10.7150/thno.27891

Ge, Q., Zhou, Y., Lu, J., Bai, Y., Xie, X., and Lu, Z. (2014). miRNA in Plasma Exosome Is Stable under Different Storage Conditions. *Molecules* 19, 1568–1575. doi:10.3390/molecules19021568

He, C., Zheng, S., Luo, Y., and Wang, B. (2018). Exosome Theranostics: Biology and Translational Medicine. *Theranostics* 8, 237–255. doi:10.7150/thno.21945

He, W., Wang, C., Mu, R., Liang, P., Huang, Z., Zhang, J., et al. (2017). miR-21 Is Required for Anti-tumor Immune Response in Mice: An Implication for its Bi-directional Roles. *Oncogene* 36, 4212–4223. doi:10.1038/onc.2017.62

Heinemann, M. L., Ilmer, M., Silva, L. P., Hawke, D. H., Recio, A., Vorontsova, M. A., et al. (2014). Benchtop Isolation and Characterization of Functional Exosomes by Sequential Filtration. *J. Chromatogr. A* 1371, 125–135. doi:10.1016/j.chroma.2014.10.026

Herter, E. K., and Xu Landén, N. (2017). Non-Coding RNAs: New Players in Skin Wound Healing. *Adv. Wound Care* 6, 93–107. doi:10.1089/wound.2016.0711

Hoshino, A., Costa-Silva, B., Shen, T.-L., Rodrigues, G., Hashimoto, A., Tesic Mark, M., et al. (2015). Tumour Exosome Integrins Determine Organotropic Metastasis. *Nature* 527, 329–335. doi:10.1038/nature15756

Hristov, D., Rodriguez-Quijada, C., Gomez-Marquez, J., and Hamad-Schifferli, K. (2019). Designing Paper-Based Immunoassays for Biomedical Applications. *Sensors* 19, 554. doi:10.3390/s19030554

Hu, J., Wang, S., Wang, L., Li, F., Pingguan-Murphy, B., Lu, T. J., et al. (2014). Advances in Paper-Based Point-of-care Diagnostics. *Biosens. Bioelectron.* 54, 585–597. doi:10.1016/j.bios.2013.10.075

Huang, R., He, L., Li, S., Liu, H., Jin, L., Chen, Z., et al. (2020). A Simple Fluorescence Aptasensor for Gastric Cancer Exosome Detection Based on Branched Rolling Circle Amplification. *Nanoscale* 12, 2445–2451. doi:10.1039/c9nr08747h

Jeppesen, D. K., Fenix, A. M., Franklin, J. L., Higginbotham, J. N., Zhang, Q., Zimmerman, L. J., et al. (2019). Reassessment of Exosome Composition. *Cell* 177, 428–445. doi:10.1016/j.cell.2019.02.029

Jin, G., Liu, Y., Zhang, J., Bian, Z., Yao, S., Fei, B., et al. (2019). A Panel of Serum Exosomal microRNAs as Predictive Markers for Chemoresistance in Advanced Colorectal Cancer. *Cancer Chemother. Pharmacol.* 84, 315–325. doi:10.1007/s00280-019-03867-6

Kalluri, R., and LeBleu, V. S. (2020). The Biology, Function, and Biomedical Applications of Exosomes. *Science* 367, eaau6977. doi:10.1126/science.aau6977

Kumar, A., Kim, S., Su, Y., Sharma, M., Kumar, P., Singh, S., et al. (2021). Brain Cell-Derived Exosomes in Plasma Serve as Neurodegeneration Biomarkers in Male Cynomolgus Monkeys Self-Administrating Oxycodone. *EBioMedicine* 63, 103192. doi:10.1016/j.ebiom.2020.103192

Lee, J., Kwon, M. H., Kim, J. A., and Rhee, W. J. (2018). Detection of Exosome miRNAs Using Molecular Beacons for Diagnosing Prostate Cancer. *Artif. Cell Nanomedicine, Biotechnol.* 46, S52–S63. doi:10.1080/21691401.2018.1489263

Lee, J., Kim, H., Heo, Y., Yoo, Y. K., Han, S. I., and Kim, C. (2020). Enhanced Paper-Based Elisa for Simultaneous EVs/Exosome Isolation and Detection Using Streptavidin Agarose-Based Immobilization. *Analyst* 145, 157–164. doi:10.1039/C9AN01140D

Li, W., Li, C., Zhou, T., Liu, X., Liu, X., Li, X., et al. (2017). Role of Exosomal Proteins in Cancer Diagnosis. *Mol. Cancer* 16, 145. doi:10.1186/s12943-017-0706-8

Li, Y., Zheng, Q., Bao, C., Li, S., Guo, W., Zhao, J., et al. (2015). Circular RNA Is Enriched and Stable in Exosomes: A Promising Biomarker for Cancer Diagnosis. *Cell Res* 25, 981–984. doi:10.1038/cr.2015.82

Liu, Q., Zhang, H., Jiang, X., Qian, C., Liu, Z., and Luo, D. (2017). Factors Involved in Cancer Metastasis: A Better Understanding to "Seed and Soil" Hypothesis. *Mol. Cancer* 16, 176. doi:10.1186/s12943-017-0742-4

Logozzi, M., Angelini, D. F., Iessi, E., Mizzoni, D., Di Raimo, R., Federici, C., et al. (2017). Increased PSA Expression on Prostate Cancer Exosomes in *In Vitro* Condition and in Cancer Patients. *Cancer Lett.* 403, 318–329. doi:10.1016/j.canlet.2017.06.036

Logozzi, M., Mizzoni, D., Angelini, D., Di Raimo, R., Falchi, M., Battistini, L., et al. (2018). Microenvironmental pH and Exosome Levels Interplay in Human Cancer Cell Lines of Different Histotypes. *Cancers* 10, 370. doi:10.3390/cancers10100370

Mahmoudi, T., Tazehkand, A. P., Pourhassan-Moghaddam, M., Alizadeh-Ghodsi, M., Ding, L., and Baradaran, B. (2020). PCR-Free Paper-Based Nanobiosensing Platform for Visual Detection of Telomerase Activity via Gold Enhancement. *Microchem. J.* 154, 104594. doi:10.1016/j.microc.2020.104594

Mashouri, L., Yousefi, H., Aref, A. R., Ahadi, A. M., Molaei, F., and Alahari, S. K. (2019). Exosomes: Composition, Biogenesis, and Mechanisms in Cancer Metastasis and Drug Resistance. *Mol. Cancer* 18, 75. doi:10.1186/s12943-019-0991-5

Mathieu, M., Martin-Jaular, L., Lavieu, G., and Théry, C. (2019). Specificities of Secretion and Uptake of Exosomes and Other Extracellular Vesicles for Cell-To-Cell Communication. *Nat. Cel Biol.* 21, 9–17. doi:10.1038/s41556-018-0250-9

Moridikia, A., Mirzaei, H., Sahebkar, A., and Salimian, J. (2018). MicroRNAs: Potential Candidates for Diagnosis and Treatment of Colorectal Cancer. *J. Cel. Physiol.* 233, 901–913. doi:10.1002/jcp.25801

Moscetti, I., Cannistraro, S., and Bizzarri, A. R. (2019). Probing Direct Interaction of Oncomir-21-3p with the Tumor Suppressor P53 by Fluorescence, Fret and Atomic Force Spectroscopy. *Arch. Biochem. Biophys.* 671, 35–41. doi:10.1016/j.abb.2019.05.026

Ocansey, D. K. W., Zhang, L., Wang, Y., Yan, Y., Qian, H., Zhang, X., et al. (2020). Exosome-mediated Effects and Applications in Inflammatory Bowel Disease. *Biol. Rev.* 95, 1287–1307. doi:10.1111/brv.12608

Park, J., Hwang, M., Choi, B., Jeong, H., Jung, J.-h., Kim, H. K., et al. (2017). Exosome Classification by Pattern Analysis of Surface-Enhanced Raman Spectroscopy Data for Lung Cancer Diagnosis. *Anal. Chem.* 89, 6695–6701. doi:10.1021/acs.analchem.7b00911

Parolini, I., Federici, C., Raggi, C., Lugini, L., Palleschi, S., De Milito, A., et al. (2009). Microenvironmental pH Is a Key Factor for Exosome Traffic in Tumor Cells. *J. Biol. Chem.* 284, 34211–34222. doi:10.1074/jbc.m109.041152

PinkyGupta, S., Gupta, S., Krishnakumar, V., Sharma, Y., Dinda, A. K., and Mohanty, S. (2021). Mesenchymal Stem Cell Derived Exosomes: A Nano Platform for Therapeutics and Drug Delivery in Combating Covid-19. *Stem Cel Rev Rep* 17, 33–43. doi:10.1007/s12015-020-10002-z

Qiao, L., Hu, S., Huang, K., Su, T., Li, Z., Vandergriff, A., et al. (2020). Tumor Cell-Derived Exosomes Home to Their Cells of Origin and Can Be Used as Trojan Horses to Deliver Cancer Drugs. *Theranostics* 10, 3474–3487. doi:10.7150/thno.39434

Qing, L., Chen, H., Tang, J., and Jia, X. (2018). Exosomes and Their Microrna Cargo: New Players in Peripheral Nerve Regeneration. *Neurorehabil. Neural Repair* 32, 765–776. doi:10.1177/1545968318798955

Quesada-González, D., and Merkoçi, A. (2018). Nanomaterial-based Devices for Point-of-care Diagnostic Applications. *Chem. Soc. Rev.* 47, 4697–4709. doi:10.1039/c7cs00837f

Rashid, M. H., Borin, T. F., Ara, R., Angara, K., Cai, J., Achyut, B. R., et al. (2019). Differential *In Vivo* Biodistribution of 131I-Labeled Exosomes from Diverse Cellular Origins and its Implication for Theranostic Application. *Nanomedicine: Nanotechnology, Biol. Med.* 21, 102072. doi:10.1016/j.nano.2019.102072

Romao, V. C., Martins, S. A. M., Germano, J., Cardoso, F. A., Cardoso, S., and Freitas, P. P. (2017). Lab-on-chip Devices: Gaining Ground Losing Size. *ACS Nano* 11, 10659–10664. doi:10.1021/acsnano.7b06703

Royo, F., Cossío, U., Ruiz de Angulo, A., Llop, J., and Falcon-Perez, J. M. (2019). Modification of the Glycosylation of Extracellular Vesicles Alters Their Biodistribution in Mice. *Nanoscale* 11, 1531–1537. doi:10.1039/c8nr03900c

Sengupta, J., and Hussain, C. M. (2019). Graphene and its Derivatives for Analytical Lab on Chip Platforms. *Trac Trends Anal. Chem.* 114, 326–337. doi:10.1016/j.trac.2019.03.015

Sharma, A., and Johnson, A. (2019). Exosome DNA: Critical Regulator of Tumor Immunity and a Diagnostic Biomarker. *J. Cel Physiol.* 235, 1921–1932. doi:10.1002/jcp.29153

Smith, S., Korvink, J. G., Mager, D., and Land, K. (2018). The Potential of Paper-Based Diagnostics to Meet the Assured Criteria. *RSC Adv.* 8, 34012–34034. doi:10.1039/c8ra06132g

Tian, X.-P., Wang, C.-Y., Jin, X.-H., Li, M., Wang, F.-W., Huang, W.-J., et al. (2019). Acidic Microenvironment Up-Regulates Exosomal miR-21 and miR-10b in Early-Stage Hepatocellular Carcinoma to Promote Cancer Cell Proliferation and Metastasis. *Theranostics* 9, 1965–1979. doi:10.7150/thno.30958

Tsukamoto, M., Iinuma, H., Yagi, T., Matsuda, K., and Hashiguchi, Y. (2017). Circulating Exosomal microRNA-21 as a Biomarker in Each Tumor Stage of Colorectal Cancer. *Oncology* 92, 360–370. doi:10.1159/000463387

Wan, Z., Gao, X., Dong, Y., Zhao, Y., Chen, X., Yang, G., et al. (2018). Exosome-Mediated Cell-Cell Communication in Tumor Progression. *Am. J. Cancer Res.* 8, 1661–1673. Available at: https://www.ncbi.nlm.nih.gov/pmc/articles/PMC6176174/.

Wortzel, I., Dror, S., Kenific, C. M., and Lyden, D. (2019). Exosome-Mediated Metastasis: Communication from a Distance. *Dev. Cel* 49, 347–360. doi:10.1016/j.devcel.2019.04.011

Wu, Y., Deng, W., and Klinke II, D. J. (2015). Exosomes: Improved Methods to Characterize Their Morphology, RNA Content, and Surface Protein Biomarkers. *Analyst* 140, 6631–6642. doi:10.1039/c5an00688k

Yan, S., Han, B., Gao, S., Wang, X., Wang, Z., Wang, F., et al. (2017). Exosome-Encapsulated Micrornas as Circulating Biomarkers for Colorectal Cancer. *Oncotarget* 8, 60149–60158. doi:10.18632/oncotarget.18557

Yan, W., and Jiang, S. (2020). Immune Cell-Derived Exosomes in the Cancer-Immunity Cycle. *Trends Cancer* 6, 506–517. doi:10.1016/j.trecan.2020.02.013

Zhang, Y., Liu, Y., Liu, H., and Tang, W. H. (2019). Exosomes: Biogenesis, Biologic Function and Clinical Potential. *Cell Biosci* 9, 19. doi:10.1186/s13578-019-0282-2

Zhao, J., Zhang, Y., and Zhao, G. (2015). Emerging Role of microRNA-21 in Colorectal Cancer. *Cbm* 15, 219–226. doi:10.3233/cbm-150468

Zhu, G., Yin, X., Jin, D., Zhang, B., Gu, Y., and An, Y. (2019). Paper-based Immunosensors: Current Trends in the Types and Applied Detection Techniques. *Trac Trends Anal. Chem.* 111, 100–117. doi:10.1016/j.trac.2018.09.027

Conflict of Interest: The authors declare that the research was conducted in the absence of any commercial or financial relationships that could be construed as a potential conflict of interest.

Publisher's Note: All claims expressed in this article are solely those of the authors and do not necessarily represent those of their affiliated organizations, or those of the publisher, the editors and the reviewers. Any product that may be evaluated in this article, or claim that may be made by its manufacturer, is not guaranteed or endorsed by the publisher.

Copyright © 2022 Lai, Lee, Vu, Vu, Tsai, Chen and Cheng. This is an open-access article distributed under the terms of the Creative Commons Attribution License (CC BY). The use, distribution or reproduction in other forums is permitted, provided the original author(s) and the copyright owner(s) are credited and that the original publication in this journal is cited, in accordance with accepted academic practice. No use, distribution or reproduction is permitted which does not comply with these terms.